

30 April 2016

Dear Dr. Matthew Hecht,

Please find attached our revised manuscript. In this new version, we have taken into account almost all points raised by both reviewers and we believe they have contributed to the improvement of the manuscript. In response to Dr. Xavier Capet main point, we have performed new Lagrangian experiments with a release depth according with the nitrate depletion depth. We have included a new author to the manuscript, Dr. Arthur Capet. With his helpful contribution we have analyzed the nitrate uptake along tracks depending on the light conditions from MERIS climatology. We also have changed some ambitious sentences about our results. In response to Dr. Peter Gaube comments, we have performed longer Lagrangian simulations to analyze the potential biological impact of vertical motions.

The texts highlighted in blue color in the revised manuscript show our new additions and modifications in the light of the reviewer comments.

In the following pages we present our point-by-point reply to the reviewers comments.

We look forward to the reviewers' replies

Yours faithfully,

Bàrbara Barceló on behalf of all co-authors

REVIEWER #1 (COMMENTS AND ANSWERS):

We acknowledge Dr. Xavier Capet for his review. All the comments and suggestions have been taken into account and we believe they have contributed to the improvement of the manuscript.

In the next paragraphs we present the reviewer's comments (in blue) followed by our point-by-point reply (in black).

- As discussed for example in the manuscript conclusion (p 2268 17-10), what matters is the consequence of vertical velocities in terms of introduction of nutrients into the euphotic layer. With this in mind, I do not find the experiment protocol particularly well designed. The choice of a uniform depth range for the release of the particles implies that over most of the domain particles are situated well above the euphotic layer and nutricline, in places with almost zero lateral and vertical gradients. This choice does not seem judicious because both horizontal and vertical advection will only have minute consequences on the nitrate field, hence the authors compare the relative roles of two terms that each have a negligible role in the nitrate budget (note the tuning of the colorbar in figures 6 and 7 to display some contrasts in the southwestern sector of the domain). I do not understand why the authors have not released their particles about the nutricline to obtain a fair comparison between all parts of their domain ?

REPLY: We agree with the reviewer, horizontal and vertical advection of nutrients have significant contributions where there is a preexisting gradient of nutrients. Moreover, their contribution on ecosystems starts with the advection of nutrients into the euphotic layer. The nutricline in the offshore SEP is well below the euphotic layer, while near the coast the coastal upwelling raises the nutricline. We tried to reach a commitment between not to be so far from the euphotic layer either the nutricline. Finally, we released the water parcels between 150 and 250 m, which fully includes in the east the nutricline, includes the beginning of the nutricline in the west (see new figure 2 below) and it is close to the euphotic layer. All the methodology used in this study is based on a regular release area (bins, average, rms, etc.), hence we propose to maintain this part of the paper as an

approximate estimation of the importance that vertical motion may have on tracer dispersion. In addition, we have performed a new 364 days long simulation to analyze more realistically vertical velocity implications on nitrate distribution. In this new simulation we release the particles around the nitracline estimated as the depth at which nitrate concentration is $2 \mu\text{mol l}^{-1}$ (Omand and Mahadevan, 2015).

We have changed figures 6 and 7 as the colorbar used was not appropriate. The new figures are:

Figure 6:

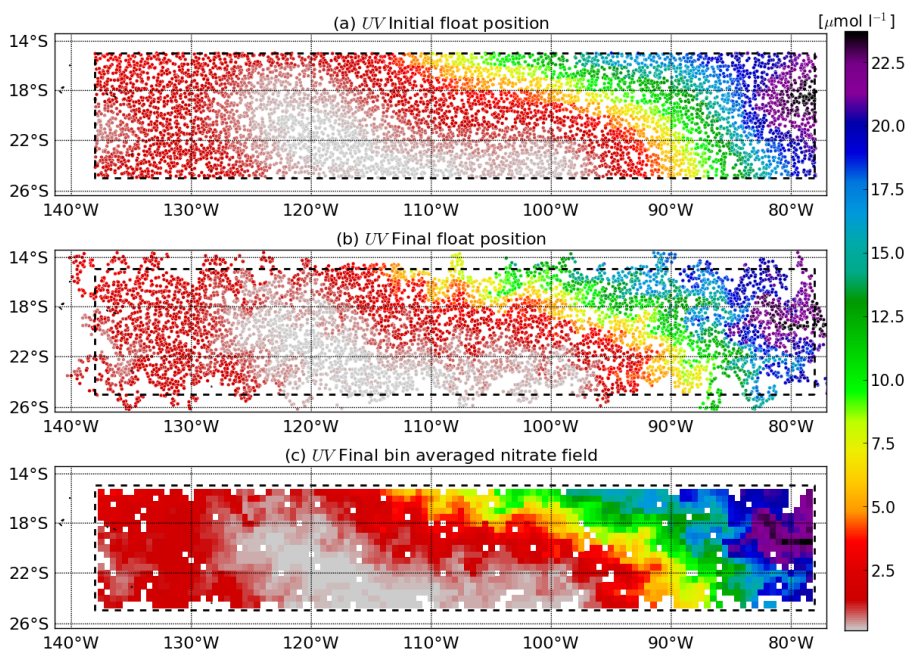
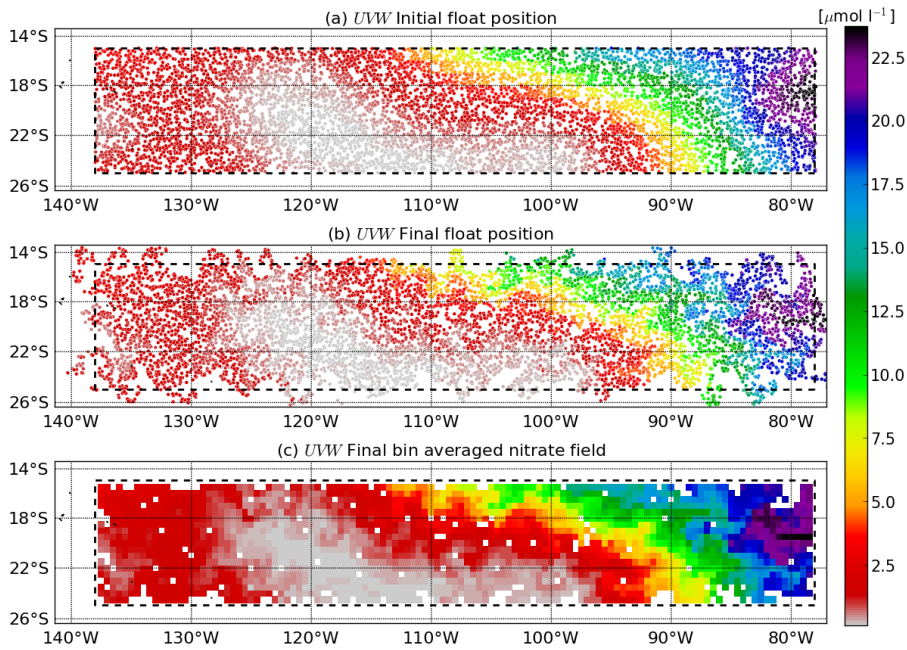
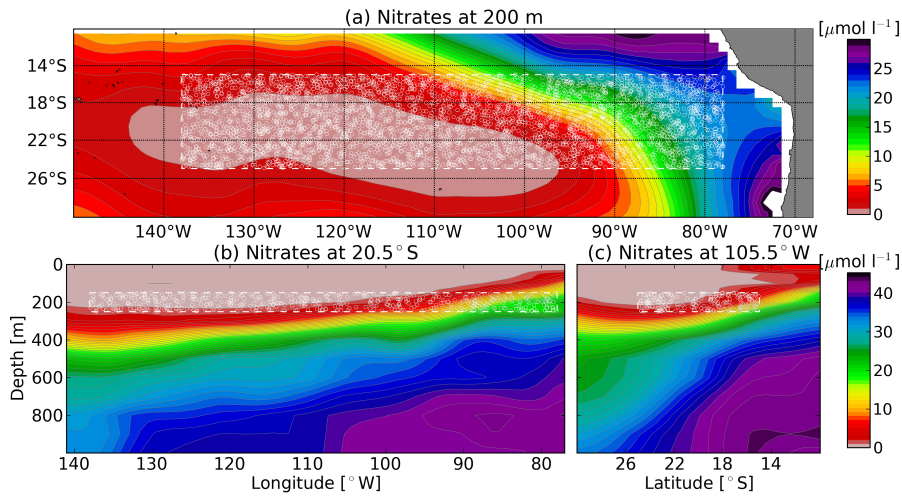


Figure 7:



And in accordance with this, we have changed figure 2 to:



- In contrast, nitrate depletion in the euphotic layer is ignored in the study whereas this term is critical to establishing some asymmetry between upward and downward nitrate fluxes. Speaking of that, a key time scale for nitrate evolution in the real ocean is that for depletion by primary production. This scale varies depending on the situation but it is frequently considered to be of the order of a few days. Although it is presumably longer in the oligotrophic SEP it is a pity that vertical velocities are weekly averaged and hence, do not resolve the presumably larger w fluctuations on time scales of one to a few days that are susceptible to interact with primary production. In the event that the authors would model the nitrate evolution with a term accounting for primary production in the upper ocean this would be a remaining limitation of their study.

REPLY: In the new long simulation the release of floats is performed at the base of the nitrate depletion layer. Through the advection of passive floats within the euphotic layer, we can estimate the evolution of the nitrate content along Lagrangian tracks considering an uptake term depending on the light conditions for each float, and a remineralization term.

We agree with Dr. Capet about the need of improving the time (and spatial) resolution of the ARMOR3D product, but this is an intrinsic limitation of the satellite observations resolution and the global coverage of the Argo program and in-situ data. Nowadays, the observation-based product is only available in $1/3^\circ$ horizontal resolution and weekly temporal resolution, and we can only perform our estimates in a mesoscale framework.

- the statement that "the vertical velocity explains about 30 % of the nitrate distribution" (p2267 lines 9 and 24) is literally false. The vertical velocities are responsible for creating nitrate variance or changes whose level after 30 days is $1/3$ of that created by horizontal advection alone. Nitrate distribution remains controlled by their initial condition to a very large degree.

REPLY: In the new version of the manuscript, we have included this clarification in the discussion of the manuscript, as well as an emphasis on the limitations of the

methodology.

- A prototypical example of the confusion that plagues the manuscript is the statement made in p2268 lines 7-14 about the fact that small vertical velocities in the SEP make an important contribution to marine ecosystem growth: "This is demonstrated by our analysis since the most important contribution of the vertical velocity on nitrate distribution is seen to be localized to the eastern part of the SEP which is characterized by moderate vertical velocity values and a high vertical nitrate gradient"). Note first that, indeed the south-eastern Pacific is the only place where particles release positions straddle the nutricline. Irrespective of the vertical velocity intensity this is thus the place where some vertical advection effects can be expected and I do not see what this proves except the fact that advection can only act on existing property gradients. In addition, the results obtained by the authors do not show nutrient injection into the euphotic layer, they show positive and negative changes in nitrate which must approximately cancel out (see the noisy red and blue patterns in Figure 8). It is only by computing fluxes that the role of vertical velocities on ecosystems can be demonstrated. On the other hand, a nutrient sink would be needed to deplete nutrients in the euphotic layer and create some asymmetry between upward and downward fluxes.

REPLY: We have carefully edited the text taking into account the reviewer's comments. With the new analysis on nitrate uptake (Section 3.3) we address the role of vertical velocities on ecosystems.

Specific comment:

p2262: dynamic height dh should be defined in the text.

REPLY: We have changed the geostrophic relation for a more self-defined formulation.

p2263: primed density should also be defined.

REPLY: primed density refers to departures from the mean density field.

p2265, lines 15-16: "Further, this result does not give any indication of the sign of the vertical motion, only its magnitude.". What sign ? The vertical velocity sign changes rapidly with time. So I do not believe that this remark is useful.

REPLY: Done, this sentence has been removed.

- rerun the particle code with releases at the same NO₃ isopleth that properly characterizes the nutricline
- keep track of the vertical excursions of the particles during their integration (which may last longer than 30 days as advocated by the 2nd reviewer). Precisely the authors could keep track of: 1) the minimum depth reached during integration 2) some form of potential production index/ based on the theoretical amount of light received during integration. Using theoretical light penetration curves decaying with depth as exponential will allow the authors to quantify the history of vertical displacements of the particles with a weighting that is relevant to the evolution of NO₃.

REPLY: The new additional long simulation aims to implement this methodology in order to estimate a realistic contribution of vertical motions on nitrate distribution. The new simulation is performed applying the methodology detailed in the new section 3.3 of the manuscript.

REVIEWER #2 (COMMENTS AND ANSWERS):

We acknowledge Dr. Peter Gaube for his review. All the specific details have been fixed. Regarding the general comments, we have also taken into account almost all of them and we consider they have contributed to the improvement of the manuscript.

In the next paragraphs we present the reviewer's comments (in blue) followed by our point-by-point reply (in black).

In my opinion, the main shortcoming of the research described in this manuscript is the short (30-day) integration time of the simulations. With only 1 month of data, it does not seem like much could really be said about the effect of mesoscale processes on nutrient distribution. For example, the average lifespan of eddies in this region exceeds 1 month (see Chelton et al., 2011a and 2011b). Furthermore, with such a short integration time, is it not a surprise that the initial and final "nitrate" are so similar (I use quotations here because the advected field is passive, which nitrate is not)? I would have run out the simulation for 300 days (at minimum) instead of running 10 ensembles, as the authors did. What exactly was the purpose of the ensemble runs anyways? I see that they report the RMS values of the "nitrate" concentration between the two experiments, but with the 10 ensembles, they should be able to provide some sort of estimates of the confidence interval of these values. This is the only reason that I can see for running the ensembles.

REPLY: We ran out the simulation in consecutive weeks in order to cover a longer period of time and to give robustness to our results. In different weeks, estimated changes on nitrate distribution caused by vertical advection are 1/3 of the horizontal advection changes. In addition, we have performed new 364 day simulations with the purpose of analyze the nitrate uptake within the euphotic layer.

I would suggest, that if the authors are interested in mesoscale differences in the nitrate distribution as a result of the inclusion of mesoscale vertical velocities, why not look at particular eddies or meanders? This could simply be done from a few case studies, or from composite analysis. A priori, the patterns of the vertical advection of nitrate in eddies is not clear. The experiment run for this project would be a great way to describe this.

REPLY: We considered this point during the construction of the manuscript. In Bàrbara's master thesis (*Quasi-geostrophic vertical motion from satellite and in-situ observations: impact on South East Pacific nitrate distribution through a Lagrangian simulation*, Section 4.2.3, available on the Research Gate) we performed a particular test case but, due to the passive advection of floats and the limitations in the extension to nitrates, we decided to discard it. On the other hand, we aim to give results valid for all the SEP with the objective of demonstrating the potential impact of vertical velocities on the advection of tracers.

A few comments: In the ARMOR3D product, is the dynamic height constrained to match observed SSH?

REPLY: Yes, the reviewer is correct. We refer to: Mulet, S.; Rio, M.-H.; Mignot, A.; Guinehut, S. & Morrow, R. A new estimate of the global 3D geostrophic ocean circulation based on satellite data and in-situ measurements. *Deep-Sea Research Part II: Topical Studies in Oceanography*, 2012, 77-80, 70-81

Page 2259, Line 21: Argo, not ARG0.

REPLY: Corrected.

Page 2260, Line 5: “..in the oligotrophic gyres mesoscale processes promote vertical advection of nutrients into the euphotic layer, thereby stimulating primary production.” Please provide a reference for this statement.

REPLY: Done. The reference is Lathuiliere, C.; Levy, M. & Echevin, V. Impact of eddy-driven vertical fluxes on phytoplankton abundance in the euphotic layer *Journal of Plankton Research*, 2011, 33, 827-831

Page 2260, Line 7: The present work is focused on the same area analyzed by Chelton et al.(2011a), the offshore South East Pacific (SEP, white box in Fig. 1), where nutrient input by mesoscale vertical exchange is considered to play a lead role in primary production.” Please provide a reference for this statement.

REPLY: Done. The reference is Lathuiliere, C.; Levy, M. & Echevin, V. Impact of eddy-driven vertical fluxes on phytoplankton abundance in the euphotic layer *Journal of Plankton Research*, 2011, 33, 827-831

Also note type of analyzed. There are numerous instances of this type. Page 2265, Line 4: With regards to the upwelling and downwelling along meanders, not that this was shown by a number of people long before Pollard and Regier, 1992. For example, look at: (Woods, 1988; Bower, 1991; Flierl and Davis, 1993; Olson et al., 1994; Spall and Richards, 2000; Lima et al., 2002), which are all included at the end of this review.

REPLY: We thank the reviewer for this remark. We have included some of these references in the revised version of the manuscript.

~~IMPACT OF VERTICAL AND HORIZONTAL ADVECTION ON NUTRIENT DISTRIBUTION IN THE SOUTH EAST PACIFIC~~ Impact of vertical and horizontal advection on nutrient distribution in the South East Pacific

Bàrbara Barceló-Llull¹, Evan Mason², Arthur Capet³, and Ananda Pascual²

¹Universidad de Las Palmas de Gran Canaria, ULPGC, Las Palmas de Gran Canaria, Spain

²Instituto Mediterráneo de Estudios Avanzados, IMEDEA (CSIC-UIB), Mallorca, Spain

³CNR, OGS, Trieste, Italy

Correspondence to: Bàrbara Barceló-Llull (b.barcelo.llull@gmail.com)

Abstract. An innovative approach is used to analyse the impact of vertical velocities associated with quasi-geostrophic (QG) dynamics on the distribution of a passive nutrient tracer (nitrate) in the South East Pacific. Twelve years of vertical and horizontal currents are derived from an observation-based estimate of the ocean state. Horizontal velocities are obtained through application of thermal
5 wind balance to weekly temperature and salinity fields. Vertical velocities are estimated by integration of the QG Omega equation. Seasonal variability of the synthetic vertical velocity and kinetic energy associated with the horizontal currents are coincident, with peaks in austral summer (November-December) in accord with published observations. Two ensembles of Lagrangian particle tracking experiments that differ according to vertical forcing ($\omega = \omega_{QG}$ versus $\omega = 0$) enable
10 a quantitative analysis of the impact of the vertical velocity. From identical initial distributions of nitrate-tagged particles, the Lagrangian results show that the impact of vertical advection on **nutrient passive tracer** distribution is 30% of the contribution of horizontal advection. An additional longer simulation analysis reveals that vertical motions are responsible for an increase in nitrate uptake of up to 30%. Despite being weaker by a factor of up to 10^{-4} than the horizontal currents, vertical
15 velocity is demonstrated to make an important contribution to nutrient distributions in the region of study.

1 Introduction

Mesoscale features make an important contribution to biogeochemical cycles through the redistribution of nutrients and passive marine organisms ~~through~~by both horizontal advection and vertical

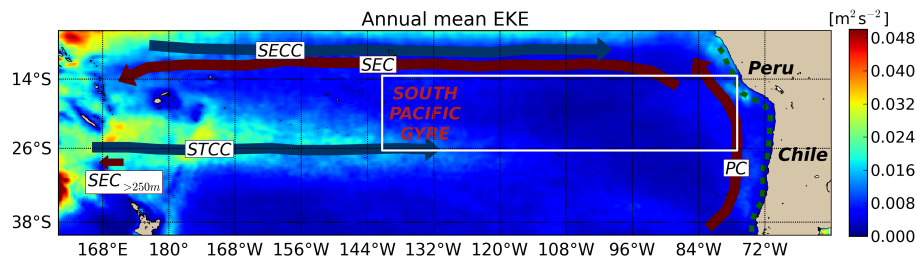


Figure 1. Map of the South East Pacific. Colours show annual mean eddy kinetic energy (EKE) computed from daily AVISO (DT14, Capet et al. (2014)) sea level anomaly data for the period 1993-2013. The white box shows the limits of the area of study. Key: SEC, South Equatorial Current; SECC, South Equatorial Countercurrent; STCC, Subtropical Countercurrent; PC, Peru Current. Green dashed line is the coastal upwelling. The small arrow indicates the poleward extent of the subsurface component of the SEC as observed by Qiu and Chen (2004) between 12-30°S at 170°E.

20 exchange. Vertical motion plays a key role in the exchange of heat, salt and biogeochemical tracers between the surface and deep ocean. In coastal upwellings, frontal areas and mesoscale eddies, the vertical velocity has fundamental importance and can significantly contribute to nutrient supply in the euphotic zone (Mahadevan, 2014).

Previous remote sensing studies (Chelton et al., 2011a) have revealed that chlorophyll-a distribu-
 25 tions within mesoscale eddies are characterized by dipole-like patterns, with extreme values found at the eddy peripheries. Chelton et al. (2011a) ~~have proposed~~ proposed that eddy horizontal advection ~~to explain this distribution~~ could explain these distributions. On the other hand, the importance of vertical exchange for phytoplankton growth and chlorophyll-a ~~distribution~~ distributions in mesoscale oceanic eddies has been attributed to various mechanisms such as eddy pumping, eddy-induced Ek-
 30 man pumping or vortex Rossby waves (McGillicuddy et al., 1998; Siegel et al., 1999; Mahadevan et al., 2012; Martin and Richards, 2001; McGillicuddy et al., 2007; Benítez-Barrios et al., 2011; Buongiorno Nardelli, 2013; Gaube et al., 2013, 2015).

In this context, we aim to quantify the importance of horizontal and vertical mesoscale motions on nutrient distribution through the application of quasi-geostrophic (QG) theory to an observation-
 35 based product (Buongiorno Nardelli et al., 2012; Pascual et al., 2015). In particular, we aim to investigate the influence of derived horizontal and vertical velocities on ocean nitrate distribution in the South East Pacific through the use of a Lagrangian particle-tracking code.

The remote South East Pacific is the least sampled oceanic region in the world ocean, in terms of both hydrography and biogeochemical structure (Ras et al., 2008). Synoptic observations from satel-
 40 lites provide crucial knowledge about such regions, despite their limitation to surface fields (Ducet et al., 2000; Dibarboure et al., 2011). The now mature ~~ARGO~~ Argo program is a source of supplementary subsurface hydrographic data (temperature and salinity) in the form of discrete vertical

profiles over a global, but sparse, grid. The ARMOR3D estimate of the ocean state (Guinehut et al., 2012) is an innovative ~~approach-product~~ where remote sensing observations (sea surface temperature and sea level anomalies) are merged with in-situ ~~ARGO-Argo~~ temperature and salinity profiles. The resulting multivariate observation-based dataset is freely available (see Section 3).

The South East Pacific has a variety of different trophic regimes (Ras et al., 2008) such as the upwelling zone near the Peru-Chile coast that is rich in nutrients and has high chlorophyll-a concentrations, and the area associated with the central part of the South Pacific Gyre, which is the most oligotrophic area in the global ocean (Morel et al., 2010). Mesoscale effects on ~~chlorophyll-a~~ chlorophyll-a production can be considered to differ between regions with different dynamical characteristics. Lathuiliere et al. (2011) demonstrate that, while mesoscale activity in upwelling regions leads primarily to offshore export of phytoplankton, in the oligotrophic gyres mesoscale processes promote vertical advection of nutrients into the euphotic layer, thereby stimulating primary production. The present work is focused on the same area analysed by Chelton et al. (2011a), the offshore South East Pacific (SEP, white box in fig. 1), where nutrient input by mesoscale vertical exchange is considered to play a lead role in primary production (Lathuiliere et al., 2011).

Figure 1 shows the time averaged eddy kinetic energy (EKE) at the surface computed from daily AVISO (DT14, Capet et al. (2014)) sea level anomalies. The EKE in the South Pacific Gyre has lower values in comparison with more active regions such as the Gulf Stream or Agulhas Current (Pascual et al., 2006; Imawaki et al., 2013). However, this gyre also includes a region with relatively high EKE values corresponding to the mid-west South Pacific. Qiu and Chen (2004) and Qiu et al. (2008) attribute the high EKE values found in this region to baroclinic instability of the eastward surface Subtropical Countercurrent (STCC) and the westward South Equatorial Current (SEC). Although the SEC is a surface current near the equator, it has a subsurface component that Qiu and Chen (2004) observed as far south as 30°S, where it underlies the STCC (see Figure 3 of Qiu and Chen (2004)). Moreover, they also find that in this region seasonal EKE modulation is related to the seasonal intensification/decay of the STCC-SEC baroclinic instability, with a maximum in November-December. In the same way, the gyre has another region with relatively high EKE values in its northwest corner. In contrast to the STCC-SEC system, Qiu and Chen (2004) attribute these high values to barotropic instabilities between the eastward South Equatorial Countercurrent (SECC) and its bordering westward SEC. The SECC-SEC system also presents seasonal EKE modulation, but with ~~maximum-maxima~~ maximum in April because the SECC-SEC horizontal shear seasonality is dominated by seasonal changes in the strength of the SECC. The two systems analysed by Qiu and Chen (2004) additionally show interannual EKE variability.

Figure 1 shows high EKE values off the Peru-Chile coast which is characterized by an important coastal upwelling and the consequent generation of mesoscale eddies and filaments (Brown et al., 2008; Brink and Robinson, 2005; Strub et al., 2013). The region of study (white box in fig. 1) is characterized by relatively low ~~eddy-kinetic-energy~~ EKE, with higher EKE values in the southwest

80 corner that are related to the STCC-SEC system ~~-, and and,~~ in the eastern section, to ~~the~~ coastal upwelling eddy generation. However, the SEP has important eddy activity due, in part, to eddy formation in the Peru-Chile coastal upwelling (Chelton et al., 2011a) .

A brief description of the synthetic temperature and salinity fields and biogeochemical data is given in section 2. Section 3 describes the methodology used to diagnose the quasi-geostrophic
85 vertical velocity, together with a description of the Lagrangian particle-tracking code ~~utilized~~ utilised for the passive nutrient simulation. In section 4 the results of the vertical velocity and kinetic energy analysis as well as the results of the Lagrangian ~~simulation~~ simulations are discussed. Section 5 summarizes and concludes the results.

2 Data

90 We use the ARMOR3D observation-based product which is based on the merging of gridded satellite sea level anomaly (SLA) and sea surface temperature (SST) remote sensing observations with in-situ vertical profiles of temperature and salinity to provide a global 3D dataset of temperature and salinity (Guinehut et al., 2012). The data are computed on a $1/3^\circ$ Mercator horizontal grid with weekly temporal resolution covering the period 1998-2009, ~~with over~~ 24 vertical levels from the
95 surface to 1500 m depth. A validation of ARMOR3D is presented by Mulet et al. (2012) who use a consistent dataset from a model reanalysis.

Auxiliary data are used to evaluate the impact of vertical and horizontal velocities on ocean nutrient distributions. Here we use climatological nitrate data from WOAPISCES (Penven et al., 2008). Nitrate data are chosen because their large vertical gradient over the mixed layer (fig. 2b and 2c)
100 highlights the contribution of vertical velocity which is characterized by smaller values than horizontal currents, but is expected to play an important role in the introduction of nutrients into the euphotic layer. Figure 2a shows the horizontal nitrate distribution at 200 m depth from WOAPISCES. High nitrate values near the Peru-Chile coast are associated with the coastal upwelling. In the zonal section (fig. 2b) the uplift of the nitracline due to the coastal upwelling off Peru-Chile coast is most
105 evident. In the meridional section (fig. 2c) nitrate concentration increases northward.

Light conditions are used in Section 4.2 to assess the relevance of the Lagrangian nitrate transport estimates. Surface Photosynthetically Active Radiation (E_0) and attenuation coefficient at 490 nm (k) are obtained from the MERIS monthly climatology (http://oceandata.sci.gsfc.nasa.gov/MERIS/Mapped/Monthly_Climatology/9km/par/, http://oceandata.sci.gsfc.nasa.gov/MERIS/Mapped/Monthly_Climatology/9km/Kd/).
110

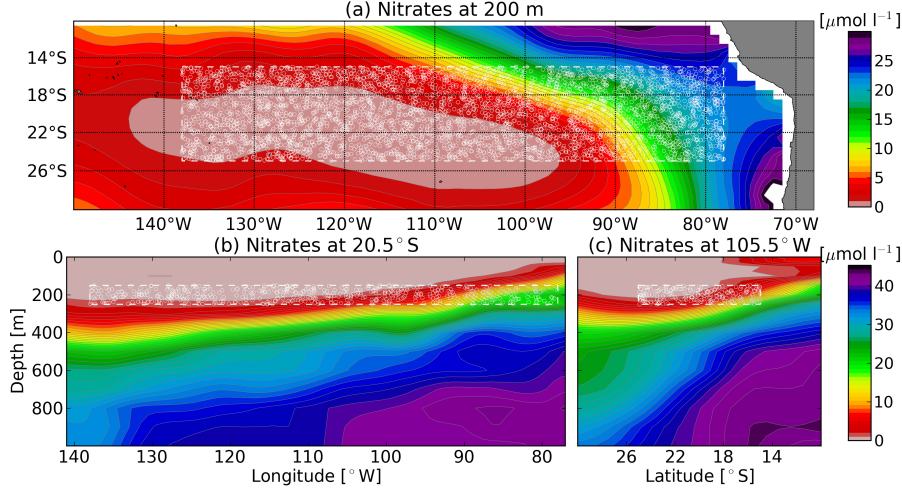


Figure 2. Climatological January mean nitrate from WOAPISCES in the South East Pacific. (a) Horizontal section at 200 m depth, (b) vertical section at 20.5°S, and (c) vertical section at 105.5°W. Discontinuous white lines delimit the Lagrangian simulation particle release area. White dots are a random sample of the simulated water parcels at their initial positions.

3 Methodology

3.1 Computation of 3D velocity

Horizontal geostrophic velocities are computed ~~through the geostrophic relation~~ at all depths z_i through the thermal wind equations:

$$115 \quad u_g(z = z_i) = u_g(z = 0) - \frac{1}{f} \frac{\partial dh}{\partial y} \frac{g}{\rho f} \int_{z=z_i}^{z=0} \frac{\partial \rho}{\partial y} dz \quad (1a)$$

$$v_g(z = z_i) = v_g(z = 0) + \frac{1}{f} \frac{\partial dh}{\partial x} \frac{g}{\rho f} \int_{z=z_i}^{z=0} \frac{\partial \rho}{\partial x} dz \quad (1b)$$

with the dynamic height, dh density, ρ , calculated from ARMOR3D temperature and salinity profiles. f is the Coriolis parameter and g is gravity.

Vertical velocity is estimated using the quasi-geostrophic approximation by integrating the QG
120 omega equation, presented here in its Q-vector formulation (Hoskins et al., 1978; Tintoré et al., 1991; Buongiorno Nardelli et al., 2012; Pascual et al., 2015):

$$N^2 \nabla_h^2 w + f^2 \frac{\partial^2 w}{\partial z^2} = 2 \nabla \cdot \mathbf{Q} \quad (2a)$$

where

$$Q = \frac{g}{\rho_0} \left(\frac{\partial v_g}{\partial x} \cdot \nabla \rho', \frac{\partial v_g}{\partial y} \cdot \nabla \rho' \right) \quad (2b)$$

125 where v_g is the geostrophic velocity vector, ~~N~~ ρ' is the departure from the mean density profile,
 N^2 the Brunt-Väisälä frequency and f the Coriolis parameter. In this implementation, ~~N~~ N^2 only
depends on depth. The Rossby number for mesoscale eddies in the SEP is generally less than 0.1
(Chelton et al., 2011b), hence we assume QG theory to be a good approximation for computing the
vertical velocity in this region.

130 Following (2), vertical velocity is estimated from density stratification and the geostrophic velocity
field. The computational code is derived following the QG vorticity and thermodynamic equations
(Buongiorno Nardelli et al., 2012). Boundary conditions are constructed by considering zero vertical
velocity at the upper, lower and lateral boundaries.

A sensitivity analysis was carried out in order to evaluate the influence of reference level choice
135 on the vertical velocity estimation. The choice of reference level is influential over the first hundred
meters above the bottom due to the imposed boundary condition; away from the bottom the same
patterns were seen for different choices of reference level (500 m and 1000 m). Testing the 500 m
reference level, the vertical velocity patterns pointed to a maximum decrease in magnitude of 50%.
Hence, a reference level of 1000 m depth was chosen. Dirichlet and Neumann conditions at the
140 lateral boundaries were tested for which we found no significant impacts on results a few points
away from the boundaries.

3.2 Lagrangian simulations

3.2.1 Passive tracer experiments

In order to analyze the respective contributions of the horizontal and vertical velocity components ~~on~~
145 to the distribution of a limiting nutrient, in Section 4.2 a Lagrangian particle-tracking code is used
to simulate water parcel trajectories forced by the derived ARMOR3D velocity fields. The tracking
code is ROMS Offline (Roff, e.g. Capet et al., 2008; Carr et al., 2008; Mason et al., 2012). Two sets of
30 day simulations were carried out for each week of 2009: the first set was forced with geostrophic
horizontal velocity and QG vertical velocity (UVW); for the second set the same geostrophic hor-
150 izontal velocity was applied but vertical velocity was set to zero (UV). Each experiment was ini-
tialised with 40000 floats placed randomly between 150-250 m depth within the study region (white
box in fig. 2). Float positions were stored every day as output of the Lagrangian simulation. Each
water parcel is tagged with the nearest value from the WOAPISCES nitrate database. ~~This nitrate
concentration value is considered a passive tracer and therefore remains~~ In these experiments, these
155 nitrate concentration values are considered as passive tracers and therefore remain unchanged with
time such that we ~~can evaluate its evolving distribution~~ only evaluate their evolving distributions
within the domain.

3.2.2 Estimates of nitrate uptake

In Section 4.2 we make an estimate of the potential biological impacts of the vertical motions derived from the ARMOR3D product through an analysis of nitrate uptake along the Lagrangian particle trajectories. To achieve this we make additional Lagrangian experiments, again using forcing by UVW and UV , where 1000 passive floats were released every week over a period of 364 days (initial date 31/12/2008) within a release area determined by the nitrate depletion depth. This depth was determined for each week following Omand and Mahadevan (2015), by selecting the depth at which nitrate content is $2\mu\text{M}$ from temporally and vertically interpolated climatological nitrate fields (WOAPISCES).

The initial nitrate concentrations for each float, $N(\mathbf{r}(t_0), t_0)$ with $\mathbf{r}(t) = (x(t), y(t), z(t))$, are interpolated in time and space from the monthly WOAPISCES climatology. In this way, the particles in each weekly release were initialized with local nutrient concentrations. The evolution of the nitrate content is then estimated along the Lagrangian tracks by considering an uptake term that is dependent on the evolving light conditions for each float (Mahadevan, 2014), and a remineralisation term:

$$\frac{\partial N}{\partial t} = -u \cdot E \cdot N + R. \quad (3)$$

The first term on the right hand part of the equation represents the uptake: u is an uptake coefficient [$(\text{Em}^{-2})^{-1}$] and the light conditions $E(\mathbf{r}(t), t) = E_0(\mathbf{r}(t), t) \cdot e^{-k \cdot z(t)}$ are derived along each track by interpolation in time and space from the MERIS monthly climatology of surface Photosynthetically Active Radiation (E_0) and attenuation coefficient at 490 nm (k) (Marra et al., 2014). The second term represents remineralization which is roughly represented by a relaxation toward climatological nitrate values whenever the actual float N content falls below the level:

$$R(\mathbf{r}(t), t) = \max\left(0, \frac{N_C - N}{r}\right), \quad (4)$$

where N_C is the climatological nitrate field (WOAPISCES), and r is a characteristic relaxation timescale [d]. This second term mainly serves to avoid too rapid depletion.

4 Results

4.1 QG vertical velocity and kinetic energy from observation-based product

A comparison between vertical velocity, w , and kinetic energy (KE) computed from the ARMOR3D derived geostrophic velocities is carried out in order to evaluate their relationship. An energetic region with high vertical velocities and mesoscale eddy activity is located in the southwest of the SEP, in both the vertical velocity (fig. 3a) and kinetic energy (fig. 3c) maps. This high eddy energy

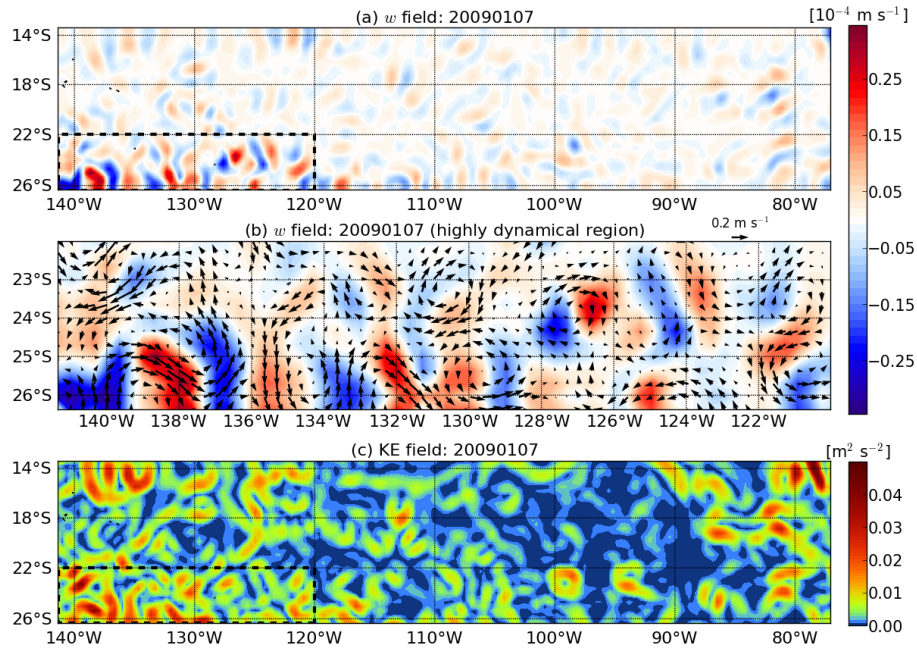


Figure 3. (a) Vertical velocity on 7 January 2009 at 200 m depth. Black box delimits the region of high mesoscale eddy activity. (b) Zoom of vertical velocity and horizontal geostrophic currents over the high mesoscale eddy activity region in (a). (c) Kinetic energy on 7 January 2009 at 200 m depth.

is related to baroclinic instabilities associated with the eastward surface Subtropical Countercurrent (STCC) and the westward underlying South Equatorial Current (SEC) system (Qiu and Chen, 2004; Qiu et al., 2008). Figure 3c shows other regions with elevated mesoscale activity that ~~is~~ are associated with less intense vertical velocity values. These regions are the coastal upwelling and the SECC-SEC system explained in section 1.

Vertical velocity in the energetic region in the southwest is highlighted in the zoom in figure 3b. Intense vertical motions of order $2-3 \text{ m day}^{-1}$ with alternating signs are located along meanders and inside eddies. The mesoscale eddies are characterized by dipole-like patterns with upwelling and downwelling cells at the eddy peripheries (e.g., $126-128^\circ \text{W}$ and $23-25^\circ \text{S}$). Vertical velocity around anticyclonic meanders (e.g., $136-139^\circ \text{W}$ and $24-26^\circ \text{S}$ or $120-122^\circ \text{W}$ and $24-26^\circ \text{S}$) shows the expected upwellings in the upstream and downwellings in the downstream portions of the meander crests (Pollard and Regier, 1992; Pascual et al., 2015) (Woods, 1988; Bower, 1991; Pollard and Regier, 1992; Pascual et al., 2015). Similarly, downwellings and upwellings in cyclonic meanders (e.g., $137-140^\circ \text{W}$ and $24.5-26^\circ \text{S}$) are located upstream and downstream of the crest, respectively.

In order to analyse the variability of w , the standard deviation over the period 7 January 1998 to 30 December 2009 is computed and shown in figure 4a. In the same way, figure 4b shows the standard deviation of the KE. The active region in the southwest of the SEP also presents high temporal

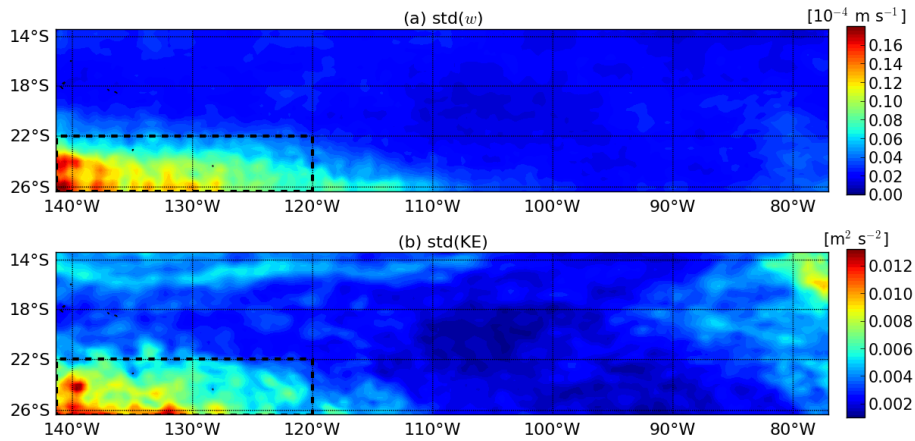


Figure 4. (a) Standard deviation of vertical velocity and (b) kinetic energy over the period 7 January 1998 to 30 December 2009 at 200 m depth. The discontinuous line delimits the region of high mesoscale variability.

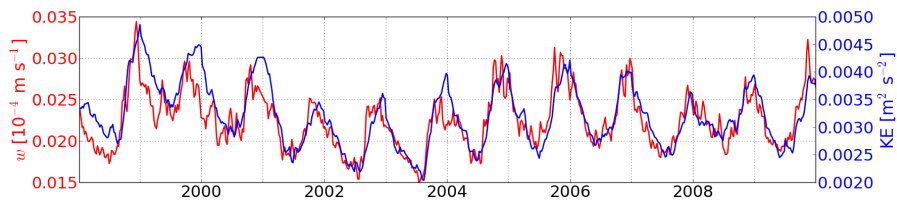


Figure 5. Time series of vertical velocity magnitude (red line) and kinetic energy (blue line) averaged over the area of study. The correlation coefficient between vertical velocity and kinetic energy is 0.84.

205 variability in both fields. The correlation coefficient between both fields in this region reaches 0.85. Considering the whole area of study the correlation coefficient is 0.79. It should be noted that this high correlation between the two variables could not be anticipated a priori as the relationship is not linear (see equations 2). ~~Further, this result does not give any indication of the sign of the vertical motion, only its magnitude.~~

210 Time series of spatial averages of vertical velocity magnitude and kinetic energy are shown in figure 5. There is clear seasonal variability in both variables, with maximums in austral summer and minimums in austral winter related to the seasonal intensification/decay of the STCC-SEC vertical shear and, in consequence, with the increase/decrease of baroclinic instability (Qiu et al., 2008). Interannual variability and weak variability of high frequency are also shown in these figures. When
 215 averaging over only the highly energetic region in the southwest (not shown) the tendency is similar but the magnitude is double.

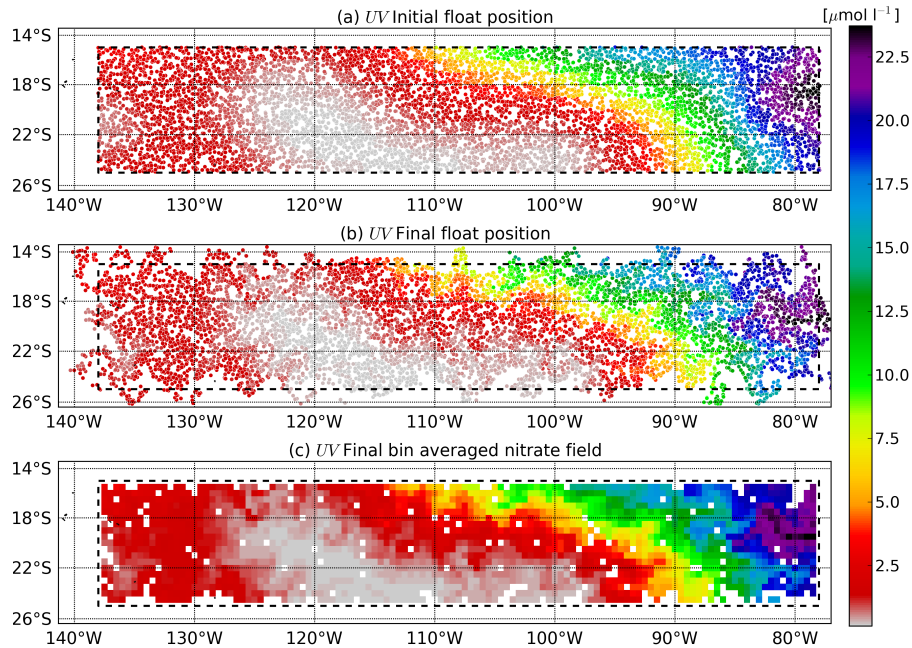


Figure 6. *UV* simulation (31/12/2008). (a) Initial positions of water parcels between 190 and 210 m depth and associated nitrate concentrations. (b) Positions of water particles between 190 and 210 m depth and associated nitrate concentrations after 30 days of forcing by geostrophic horizontal velocity and zero vertical velocity. (c) Final nitrate field computed by bin averaging the nitrate tagged fluid parcels over a $0.5^\circ \times 0.5^\circ$ grid after 30 days of simulation. Black box delimits the analysed area.

4.2 Lagrangian simulations

Figure 6a shows the initial positions of water parcels located between 190 and 210 meters depth, and their associated passive trace nitrate values. The same water parcels are advected for both the *UV* and *UVW* simulations in order to properly compare the two cases (see fig. 7a). After 30 days of simulation, the water parcels are located in new positions due to the corresponding velocity forcing (fig. 6b and 7b). The initial (not shown) and advected (fig. 6c and 7c) nitrate fields are obtained by bin averaging the nitrate tagged water parcels over a $0.5^\circ \times 0.5^\circ$ grid at the beginning and end of the respective simulations.

Figures 6c and 7c illustrate how the initially smooth nitrate field is modified by (i) the horizontal velocity (*UV* simulation) and (ii) the total velocity (*UVW* simulation) fields, respectively. Small scale structures are formed during the 30 days of simulation, with small differences arising as a result of the vertical velocity contribution. To better see these differences and to quantify the influence of horizontal and vertical motions in the Lagrangian simulations separately, anomalies are computed (see equations 5). For the *UV* simulation, subtracting the initial nitrate field from the final nitrate field gives an indication of the contribution of the horizontal velocity to the final nitrate distribution,

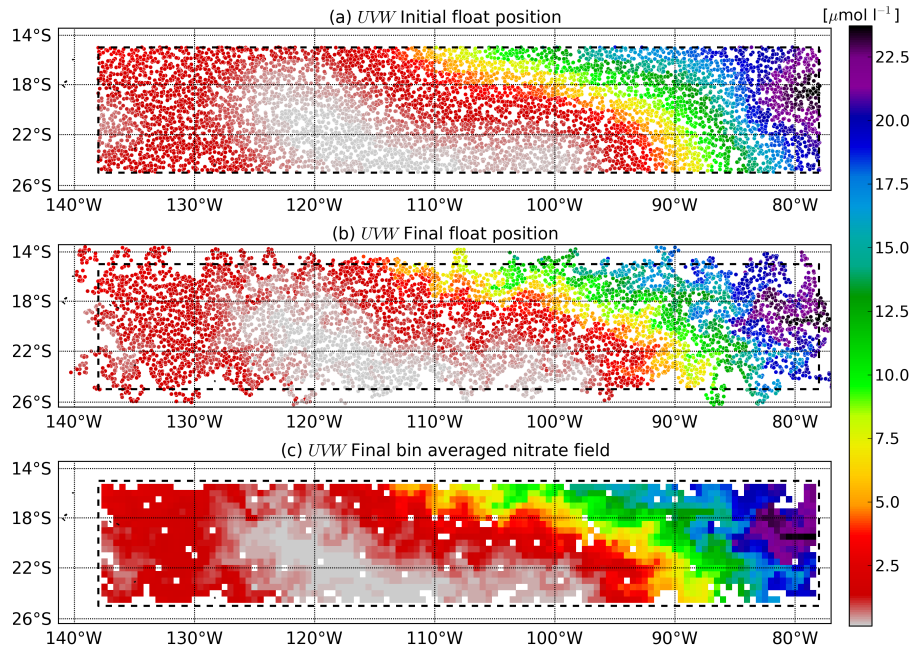


Figure 7. *UVW* simulation (31/12/2008). (a) Initial positions of water parcels between 190 and 210 m depth and associated nitrate concentrations. (b) Positions of water particles between 190 and 210 m depth and associated nitrate concentrations after 30 days of forcing by geostrophic horizontal velocity and QG vertical velocity. (c) Final nitrate field computed by bin averaging the nitrate tagged fluid parcels located over a $0.5^\circ \times 0.5^\circ$ grid after 30 days of simulation. Black box delimits the analysed area.

i.e., the anomaly aUV (fig. 8b). In the same way, the anomaly $aUVW$ (fig. 8a) gives an indication of the contribution of the total velocity. By subtracting the horizontal anomaly aUV from the total anomaly $aUVW$, the contribution of the vertical velocities, i.e., the anomaly aW can be isolated (fig. 8c).

$$aUV = UV(t_{end}) - UV(t_{ini}), \quad (5a)$$

$$aUVW = UVW(t_{end}) - UVW(t_{ini}), \quad (5b)$$

$$aW = aUVW - aUV \quad (5c)$$

Figures 8a and 8b present small differences because of the vertical velocity contribution which are highlighted in figure 8c. Although the anomalies due to vertical ~~velocity~~ velocities are smaller than aUV and $aUVW$, they are not negligible. The vertical velocity has the highest contribution off coastal upwelling zone because the moderate vertical velocity values characteristic of the eastern part of the SEP act on an important vertical nitrate gradient (see fig. 2b) caused by the uplift of the nitracline due to the coastal upwelling. On the other hand, on the southwestern part of the SEP,

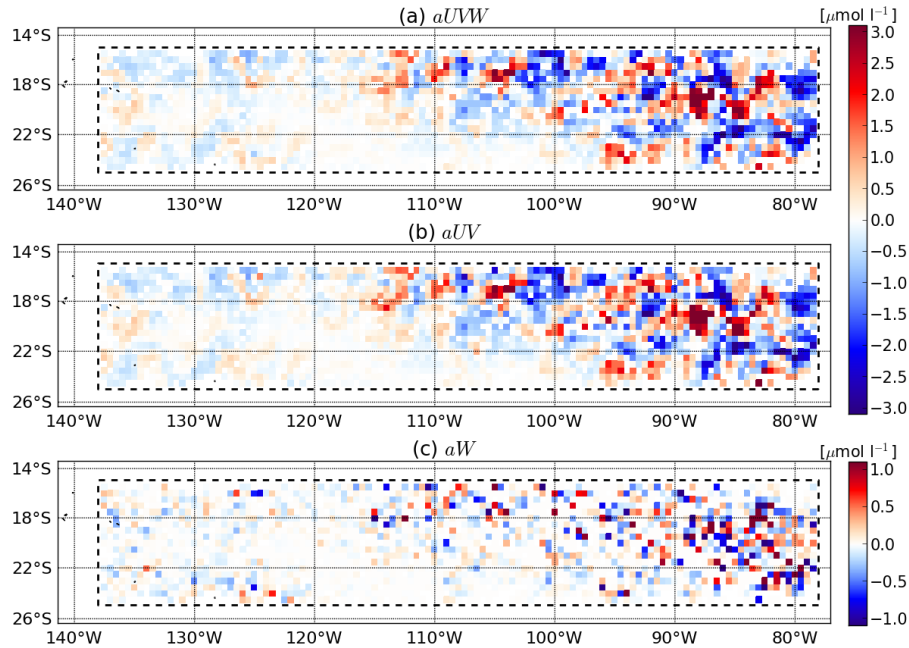


Figure 8. (31/12/2008 simulation) Nitrate anomalies resulting from (a) contributions from both QG vertical velocity and geostrophic horizontal velocity ($aUVW$); (b) the contribution from only geostrophic horizontal velocity (aUV); and (c) the QG vertical velocity contribution (aW).

245 characterized by higher dynamic activity, vertical velocity has low contribution due to the deeper nitracline.

The same procedure is performed for a total ensemble of 10 simulations in order to obtain robust results. The 30 day simulations are initialized over consecutive weeks: 31/12/2008, 07/01/2009, 14/01/2009, etc. Table 1 shows the root mean square of aUV ($rmsN_H$) and aW ($rmsN_V$). This statistical parameter provides a measure of the variability in the anomaly fields. The variability of the anomaly explained by the horizontal velocity has values ranging from 0.849 to 1.007 $\mu\text{mol l}^{-1}$, i.e., the $rmsN_H$ range of values is consistent in all simulations. The variability of aW is approximately 0.3 $\mu\text{mol l}^{-1}$ in all simulations. We can therefore assume that the vertical velocity explains approximately is responsible for creating nitrate variance whose level after 30 % of the nitrate distributions observed in our experiments days is 1/3 of that created by horizontal advection alone.

260 In order to compare the nitrate uptake rates in the Lagrangian simulations including (UVW) or excluding (UV) vertical motions, we computed the median of the nitrate uptake terms in bins of $0.5^\circ \times 0.5^\circ$ over the full annual simulations. The deeper parts of the particle trajectories, where uptake terms were lower than 0.001 [$\text{mmol N m}^{-2} \text{d}^{-1}$], were disregarded in these computations. As expected, nitrate uptake rates (Fig. 9) are higher in the upwelling region and, to a lesser extent,

Simulation	$rmsN_H$ [$\mu\text{mol l}^{-1}$]	$rmsN_V$ [$\mu\text{mol l}^{-1}$]
31/12/2008	0.851	0.321
07/01/2009	0.849	0.341
14/01/2009	0.884	0.345
21/01/2009	0.900	0.322
28/01/2009	0.912	0.338
04/02/2009	0.952	0.311
11/02/2009	1.007	0.370
18/02/2009	1.007	0.315
25/02/2009	0.971	0.302
04/03/2009	0.959	0.380

Table 1. Root mean squares of aUV ($rmsN_H$) and aW ($rmsN_V$) from the Lagrangian experiments.

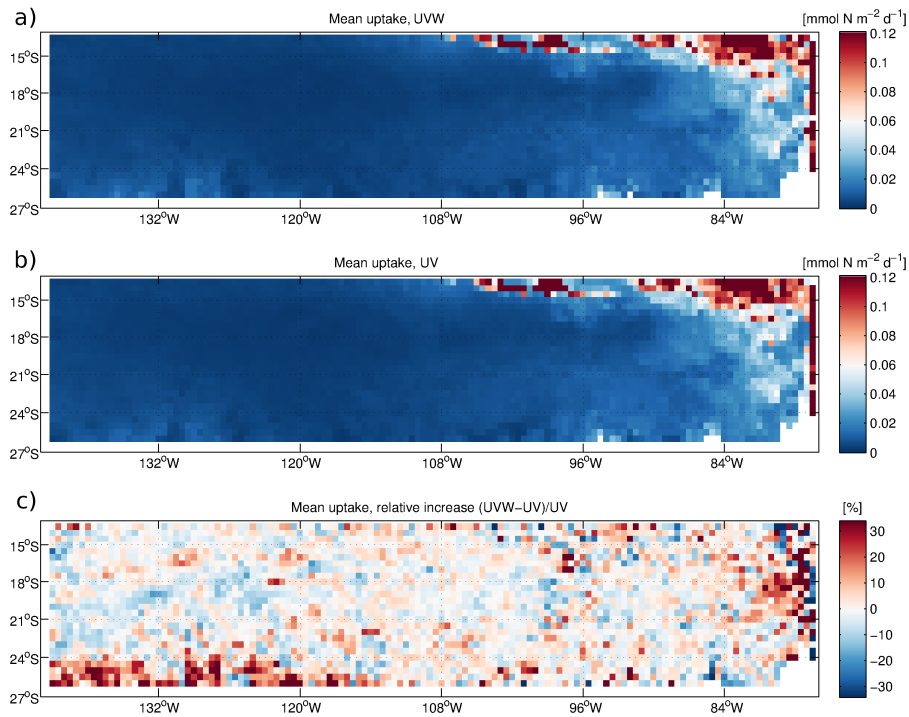


Figure 9. Nitrate uptake rates considering (a) both QG vertical velocity and geostrophic horizontal velocity (UVW); (b) only geostrophic horizontal velocity (UV); (c) Relative increase of nitrate uptake rates when including vertical velocity.

in the region of high mesoscale activity (ca. 120-140°W and 22-26°S). While the restricted resolved vertical velocities leave the overall pattern of nitrate uptake unchanged, the relative increase in the region of high mesoscale activity reaches up to 30% (Fig. 9c).

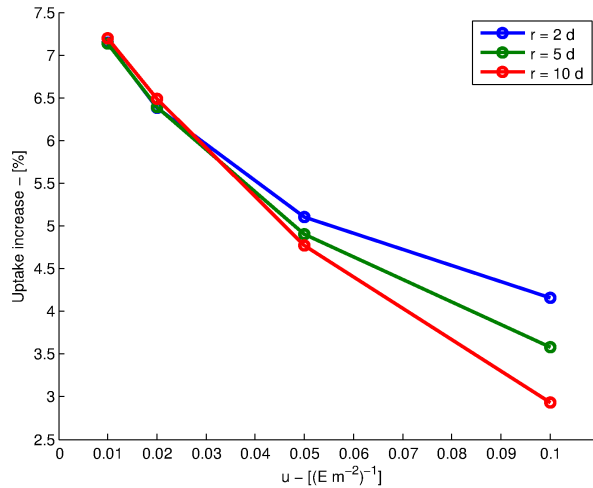


Figure 10. Averaged increase of nitrate uptake rates in the region of high mesoscale eddy activity (ca. 120-140°W and 22-26°S) for different values of the uptake coefficient u , and relaxation time scale r .

265 The simplified nutrient model used here is not suitable for a detailed study of the dynamics of nitrate. However, to demonstrate that the chosen nitrate uptake terms do return reasonable results, we tested the sensitivity of the model to changes in the u and r parameters. In Figure 10 we show that increases in spatially-averaged uptake rates over the region of high mesoscale activity vary between 3 and 7%, depending on different parameter value choices.

270 5 Discussion and Conclusions

This paper analyses vertical velocities associated with QG dynamics as derived through an innovative approach that uses the ARMOR3D global observation-based product. Weekly horizontal geostrophic velocity and QG vertical velocity are computed from ARMOR3D temperature and salinity in the South East Pacific. Two groups of Lagrangian simulations are forced with these 3D velocity fields. One group of simulations uses the 3D geostrophic velocities and QG vertical velocity in order to evaluate their combined contribution to nitrate distribution. The second group of simulations is forced with 3D geostrophic velocities with zero vertical velocity in order to evaluate the horizontal velocity contribution to the nitrate distribution. With these respective contributions, we isolate the QG vertical velocity contribution to nitrate distribution. With the root mean square statistical parameter, we obtain an estimate of nitrate distribution variability that can be explained by QG vertical velocity. ~~In comparison with the horizontal velocity contribution, the vertical velocity explains about~~ The QG vertical velocity is responsible for creating nitrate variances whose levels after 30 % of the nitrate distribution days is 1/3 of that created by horizontal advection alone. In support of this result, a ~~sensitivity analysis produced~~ series of sensitivity analyses produce similar

285 values. ~~Although we only analyse the mesoscale vertical velocity, the importance of submesoscale features on vertical tracer dispersion has been shown by (Klein and Lapeyre, 2009). Because of this, the vertical velocity contribution estimated here can be considered an underestimation of the real vertical velocity contribution. Fine resolution satellite observations can help to better evaluate the impact of vertical motion on nutrient distribution. The wide-swath SWOT altimeter will allow~~
290 ~~unique observations in the 15–100 km range of wavelength scales when it comes online in the next decade (Fu and Ferrari, 2008).~~

We ~~have also analysed~~ also analyse the QG vertical velocity in order to understand its distribution. The southwest of the SEP has relatively high mesoscale activity with vertical velocities exceeding 2 m day^{-1} , which is on the order of 10^{-4} times the horizontal velocity. Despite ~~its relatively~~
295 ~~small magnitude, the vertical velocity makes an important contribution to marine ecosystem growth through~~ their relatively small magnitudes, vertical motions may have an important impact on the introduction of nutrients into the euphotic layer in areas with pre-existing vertical gradient of nutrients and, hence, can be considered influential on marine ecosystem variability. Using a Lagrangian approach, we provide a simple demonstration of this by estimating spatial changes in nitrate distributions
300 due to vertical and horizontal advection below the euphotic layer. In the depth layer analysed (150–250 m), with weekly fields and considering the QG approximation, we find that vertical velocities contribute to these changes in 1/3 of the changes created by the horizontal advection. Despite being orders of magnitude smaller than their horizontal counterparts, this demonstrates that vertical velocities are influential in the redistribution of nutrients. Additional Lagrangian experiments within the euphotic
305 layer enable an examination of nitrate uptake rates under varying light conditions. These additional analyses reveal that vertical motions may be responsible for increases in nitrate uptake rates of up to 30%. Although this is a stimulating result, we caution that the nitrate model used is simple and highly dependent on the parameter choices for the nitrogen uptake coefficient (u) and relaxation timescale (r). We therefore consider this result as an indicator of the importance that vertical motion
310 may have on nutrient redistribution. ~~This is demonstrated by our analysis since the most important contribution of the vertical velocity on nitrate distribution is seen to be localized to the eastern part of the SEP which is characterized by moderate vertical velocity values and a high vertical nitrate gradient.~~

An additional result obtained from the QG vertical velocity and kinetic energy analysis is that vertical velocity and kinetic energy in the SEP have similar and intense seasonal variability with maximums in austral summer (November–December), which suggests that these quantities are mostly influenced by the seasonal modulation of STCC-SEC vertical shear (Qiu and Chen, 2004; Qiu et al., 2008).

Although we only analyse the mesoscale vertical velocity, the importance of submesoscale features on vertical tracer dispersion has been shown by Klein and Lapeyre (2009). Accordingly, the vertical velocity contribution estimated here can be considered an underestimation of the real vertical velocity

contribution. Fine resolution satellite observations can help to better evaluate the impact of vertical motions on nutrient redistribution. The wide-swath SWOT altimeter will allow unique observations in the 15-100 km range of wavelength scales when it comes online in the next decade (Fu and Ferrari, 2008).

325

Acknowledgements. This work has been carried out as part of E-MOTION (CTM2012-31014) project funded by the Spanish National Research Program. Additional funding from the Local Government of the Balearic Islands (CAIB-51/2011 grant) is also acknowledged. Bàrbara Barceló-Llull is supported by a pre-doctoral grant from the Spanish National Research Program associated to the PUMP (CTM2012-33355) project. Evan Mason is supported by a post-doctoral grant from the Conselleria d'Educació, Cultura i Universitats del Govern de les Illes Balears (Mallorca, Spain) and the European Social Fund. Arthur Capet is funded by the European Union under FP7- People-Co-funding of Regional, National and International Programmes, GA n. 600407. The ARMOR3D dataset was produced by CLS with support from MyOcean project (EU N° FP7-SPACE-2007-1-Grant Agreement 218812). Nitrate data were extracted from the WOAPISCES biogeochemical climatology

335 .

References

- Benítez-Barrios, V., Pelegrí, J. L., Hernández-Guerra, A., Lwiza, K. M. M., Gomis, D., Vélez-Belchí, P., and Hernández-León, S.: Three-dimensional circulation in the NW Africa coastal transition zone, *Prog. Oceanogr.*, 91, 516–533, doi:10.1016/j.pocean.2011.07.022, 2011.
- 340 Bower, A. S.: A simple kinematic mechanism for mixing fluid parcels across a meandering jet, *J. Phys. Oceanogr.*, 21, 173–180, 1991.
- Brink, K. H. and Robinson, A. R., eds.: *The Sea, Volume 11: The Global Coastal Ocean: Regional Studies and Syntheses*, Harvard University Press, 2005.
- Brown, S. L., Landry, M. R., Selph, K. E., Jin Yang, E., Rii, Y. M., and Bidigare, R. R.: Diatoms in the desert: 345 Plankton community response to a mesoscale eddy in the subtropical North Pacific, *Deep-Sea Res.*, 55, 1321–1333, doi:10.1016/j.dsr2.2008.02.012, 2008.
- Buongiorno Nardelli, B.: Vortex waves and vertical motion in a mesoscale cyclonic eddy, *J. Geophys. Res. Oceans*, 118, 5609–5624, 2013.
- Buongiorno Nardelli, B., Guinehut, S., Pascual, A., Drillet, Y., Ruiz, S., and Mulet, S.: Towards high resolution 350 mapping of 3-D mesoscale dynamics from observations, *Ocean Sci.*, 8, 885–901, 2012.
- Capet, A., Mason, E., Rossi, V., Troupin, C., Faugère, Y., Pujol, I., and Pascual, A.: Geophysical Research Letters Volume 41, Issue 21, 16 November 2014, Pages 7602-7610 Implications of refined altimetry on estimates of mesoscale activity and eddy-driven offshore transport in the Eastern Boundary Upwelling Systems, *J. Geophys. Res. Lett.*, 41, 7602–7610, doi:10.1002/2014GL061770, 2014.
- 355 Capet, X. J., Campos, E. J., and Paiva, A. M.: Submesoscale activity over the Argentinian shelf, *J. Geophys. Res. Lett.*, 35, L15605, doi:10.1029/2008GL034736, 2008.
- Carr, S. D., Capet, X. J., McWilliams, J. C., Pennington, J. T., and Chavez, F. P.: The influence of diel vertical migration on zooplankton transport and recruitment in an upwelling region: estimates from a coupled behavioral-physical model, *Fish. Oceanogr.*, 17, 1–15, doi:10.1111/j.1365-2419.2007.00447.x, 2008.
- 360 Chelton, D. B., Gaube, P., Schlax, M. G., Early, J. J., and Samelson, R. M.: The Influence of Nonlinear Mesoscale Eddies on Near-Surface Oceanic Chlorophyll, *Science*, 334, 328–332, 2011a.
- Chelton, D. B., Schlax, M. A., and Samelson, R. M.: Global observations of nonlinear mesoscale eddies, *Prog. Oceanogr.*, 91, 167–216, doi:10.1016/j.pocean.2011.01.002, 2011b.
- Dibarboure, G., Pujol, M.-I., Briol, F., Le Traon, P.-Y., Larnicol, G., Picot, N., Mertz, F., and Ablain, M.: 365 Jason-2 in DUACS: Updated system description, first tandem results and impact on processing and products, *Marine Geodesy*, 34, 214–241, 2011.
- Ducet, N., Le Traon, P.-Y., and Reverdin, G.: Global high-resolution mapping of ocean circulation from TOPEX/Poseidon and ERS-1 and -2, *J. Geophys. Res.*, 105, 19 477–19 498, 2000.
- Fu, L.-L. and Ferrari, R.: Observing Oceanic Submesoscale Processes From Space, *Eos Trans. AGU*, 89, 370 488–488, 2008.
- Gaube, P., Chelton, D. B., Strutton, P. G., and Behrenfeld, M. J.: Satellite observations of chlorophyll, phytoplankton biomass, and Ekman pumping in nonlinear mesoscale eddies, *Journal of Geophysical Research*, 118, 6349–6370, 2013.
- Gaube, P., Chelton, D. B., Samelson, R. M., Schlax, M. G., and O’neill, L. W.: Satellite Observations of 375 Mesoscale Eddy-Induced Ekman Pumping, *J. Phys. Oceanogr.*, 2015.

- Guinehut, S., Dhomps, A.-L., Larnicol, G., and Le Traon, P.-Y.: High resolution 3-D temperature and salinity fields derived from in situ and satellite observation, *Ocean Sci.*, 8, 845–857, 2012.
- Hoskins, B. J., Draghici, I., and Davies, H. C.: A new look at the ω -equation, *Quart. J. R. Met. Soc.*, 104, 31–38, 1978.
- 380 Imawaki, S., Bower, A. S., Beal, L., and Qiu, B.: Chapter 13 - Western Boundary Currents, in: *Ocean Circulation and Climate A 21st Century Perspective*, edited by Gerold Siedler, Stephen M. Griffies, J. G. and Church, J. A., vol. 103 of *International Geophysics*, pp. 305 – 338, Academic Press, doi:<http://dx.doi.org/10.1016/B978-0-12-391851-2.00013-1>, <http://www.sciencedirect.com/science/article/pii/B9780123918512000131>, 2013.
- 385 Klein, P. and Lapeyre, G.: The Oceanic Vertical Pump Induced by Mesoscale and Submesoscale Turbulence, *Annu. Rev. Marine Sci.*, 1, 351–375, doi:10.1146/annurev.marine.010908.163704, 2009.
- Lathuiliere, C., Levy, M., and Echevin, V.: Impact of eddy-driven vertical fluxes on phytoplankton abundance in the euphotic layer, *Journal of Plankton Research*, 33, 827–831, 2011.
- Mahadevan, A.: Eddy effects on biogeochemistry, *Nature*, 506, 168–169, 2014.
- 390 Mahadevan, A., D’Asaro, E., Lee, C., and Perry, M. J.: Eddy-driven stratification initiates North Atlantic spring phytoplankton blooms, *Science*, 336, 54–58, 2012.
- Marra, J. F., Lance, V. P., Vaillancourt, R. D., and Hargreaves, B. R.: Resolving the ocean’s euphotic zone, *Deep Sea Res. Part I: Oceanographic Research Papers*, 83, 45–50, 2014.
- Martin, A. P. and Richards, K. J.: Mechanisms for vertical nutrient transport within a North Atlantic mesoscale eddy, *Deep-Sea Research Part II: Topical Studies in Oceanography*, 48, 757–773, 2001.
- 395 Mason, E., Colas, F., and Pelegrí, J. L.: A Lagrangian study tracing water parcel origins in the Canary Upwelling System, *Sci. Mar.*, 76, 79–94, doi:10.3989/scimar.03608.18D, 2012.
- McGillicuddy, D. J., Robinson, A. R., Siegel, D. A., Jannasch, H. W., Johnson, R., Dickey, T. D., McNeil, J., Michaels, A. F., and Knap, A. H.: Influence of mesoscale eddies on new production in the Sargasso Sea, 400 *Nature*, 394, 263–266, 1998.
- McGillicuddy, D. J., Anderson, L. A., Bates, N. R., Bibby, T., Buesseler, K. O., Carlson, C. A., Davis, C. S., Ewart, C., Falkowski, P. G., Goldthwait, S. A., Hansell, D. A., Jenkins, W. J., Johnson, R., Kosnyrev, V. K., Ledwell, J. R., Li, Q. P., Siegel, D. A., and Steinberg, D. K.: Eddy Wind interactions stimulate extraordinary mid-ocean plankton blooms, *Science*, 316, 1021–1026, 2007.
- 405 Morel, A., Claustre, H., and Gentili, B.: The most oligotrophic subtropical zones of the global ocean: similarities and differences in terms of chlorophyll and yellow substance, *Biogeosciences*, 7, 3139–3151, doi:10.5194/bg-7-3139-2010, 2010.
- Mulet, S., Rio, M.-H., Mignot, A., Guinehut, S., and Morrow, R.: A new estimate of the global 3D geostrophic ocean circulation based on satellite data and in-situ measurements., *Deep-Sea Research Part II: Topical Studies in Oceanography*, 77-80, 70–81, 2012.
- 410 Omand, M. M. and Mahadevan, A.: The shape of the oceanic nitracline, *Biogeosciences*, 12, 3273–3287, doi:10.5194/bg-12-3273-2015, 2015.
- Pascual, A., Faugère, Y., Larnicol, G., and Le Traon, P.-Y.: Improved description of the ocean mesoscale variability by combining four satellite altimeters, *Geophys. Res. Lett.*, 33, L02611, doi:10.1029/2005GL024633, 415 2006.

- Pascual, A., Ruiz, S., Buongiorno Nardelli, B., Guinehut, S., Iudicone, D., and Tintoré, J.: Net primary production in the Gulf Stream sustained by quasi-geostrophic vertical exchanges, *Geophys. Res. Lett.*, 2015.
- Penven, P., Marchesiello, P., Debreu, L., and Lefèvre, J.: Software tools for pre- and post-processing of oceanic regional simulations, *Environmental Modelling and Software*, 23, 660–662, 2008.
- 420 Pollard, R. T. and Regier, L. A.: Vorticity and Vertical Circulation at an Ocean Front, *J. Phys. Oceanogr.*, 22, 609–625, doi:10.1175/1520-0485(1992)022<0609:VAVCAA>2.0.CO;2, 1992.
- Qiu, B. and Chen, S.: Seasonal modulations in the Eddy Field of the South Pacific Ocean, *J. Phys. Oceanogr.*, 34, 1515–1527, doi:10.1175/1520-0485(2004)034<1515:SMITEF>2.0.CO;2, 2004.
- Qiu, B., Scott, R. B., and Chen, S.: Length Scales of Eddy Generation and Nonlinear Evolution of the Seasonally
425 Modulated South Pacific Subtropical Countercurrent, *J. Phys. Oceanogr.*, 38, 1515–1528, 2008.
- Ras, J., Claustre, H., and Uitz, J.: Spatial variability of phytoplankton pigment distributions in the Subtropical South Pacific Ocean: Comparison between in situ and predicted data, *Biogeosciences*, 5, 353–369, 2008.
- Siegel, D. A., McGillicuddy Jr., D. J., and Fields, E. A.: Mesoscale eddies, satellite altimetry, and new production in the Sargasso Sea, *Journal of Geophysical Research C: Oceans*, 104, 13 359–13 379, 1999.
- 430 Strub, P. T., Combes, V., Shillington, F. A., and Pizarro, O.: Chapter 14 - Currents and Processes along the Eastern Boundaries, in: *Ocean Circulation and Climate A 21st Century Perspective*, edited by Gerold Siedler, Stephen M. Griffies, J. G. and Church, J. A., vol. 103 of *International Geophysics*, pp. 339 – 384, Academic Press, doi:http://dx.doi.org/10.1016/B978-0-12-391851-2.00014-3, <http://www.sciencedirect.com/science/article/pii/B9780123918512000143>, 2013.
- 435 Tintoré, J., Gomis, D., Alonso, S., and Parrilla, G.: Mesoscale Dynamics and Vertical Motion in the Alborán Sea, *J. Phys. Oceanogr.*, 21, 811–823, doi:10.1175/1520-0485(1991)021<0811:MDAVMI>2.0.CO;2, 1991.
- Woods, J.: *Toward a Theory on Biological-Physical Interactions in the World Ocean*, chap. Scale Upwelling and Primary Production, pp. 7–38, Springer Netherlands, doi:10.1007/978-94-009-3023-0_2, 1988.